Investigation on radiative load ratio of chilled beams on performances of solar hybrid adsorption refrigeration system for radiant cooling in subtropical city

K.F. Fong*, C.K. Lee, T.T. Chow

Building Energy and Environmental Technology Research Unit, School of Energy and Environment & Division of Building Science and Technology, City University of Hong Kong, Hong Kong, China
** Corresponding author. Tel: +852 3442 8724, Fax: +852 3442 9716, E-mail: bssquare@cityu.edu.hk*

Abstract: The effectiveness of solar adsorption system for space conditioning would be enhanced through radiant ceiling cooling, since a higher chilled water temperature can be supplied. In such provision, desiccant dehumidification should be involved in order to cater for the latent cooling load. A solar hybrid adsorption refrigeration system is therefore formulated. In this study, the effect of radiative load ratio *R* of active chilled beams (ACB) and passive chilled beams (PCB) for the solar hybrid adsorption refrigeration system was investigated. Through the year-round dynamic simulation, it was found that the performances, like solar fraction and primary energy consumption, of the system with ACB or PCB would be improved along with the decrease of *R* from 0.3 to 0.1. At the same *R*, the system with PCB would have better performances than that with ACB. With suitable design and control, the solar hybrid adsorption refrigeration system with PCB at low *R* would be more technically feasible for office use in the subtropical climate.

Keywords: *Radiant cooling, Radiative load ratio, Adsorption refrigeration, Solar air-conditioning, High temperature cooling*

1. Introduction

To promote the low energy buildings in the hot and humid places, strategic use of renewable energy in air-conditioning would certainly contribute to sustainable design. Solar air-conditioning is getting popular in the European countries [1,2]. Through the approach of high temperature cooling, the energy performance of chiller can be enhanced by using higher chilled water supply temperature for radiant cooling. As the latent cooling load cannot be effectively handled in such provision, a separate desiccant dehumidification is necessary [3,4]. In fact, it would be effective to hybridize the adsorption refrigeration, radiant cooling and desiccant dehumidification, driven by solar energy for building space conditioning. In the previous study [5], this solar hybrid adsorption refrigeration system would have much less annual primary energy consumption than the conventional vapour compression air-conditioning system for office application. In this study, it is to investigate more deeply about the effect of chilled beams on the performances of the solar hybrid adsorption refrigeration system in the subtropical city.

The common chilled beams include the active chilled beams (ACB) and passive chilled beams (PCB), which are mounted at the ceiling level but not for structural purpose. ACB have finned coils, in which chilled water flows inside. ACB make use of forced convection for cooling through induction, so they are connected with a supply air stream that is mechanically driven. PCB also have finned coils inside, but they rely on natural convection rather than forced convection. Therefore, their performances would be affected by the radiative load ratio, which is the proportion of radiative to total (i.e. radiative and convective) cooling capacity of the chilled beams. In this study, the effect of the radiative load ratio *R* on the year-round performances of the solar hybrid adsorption refrigeration system was evaluated for the office application. Two types of offices were involved, a typical office and a high-tech

office, where the latter is featured with a much higher internal heat gains due to different electrical facilities of information technology and office automation.

Fig. 1 illustrates the design of solar hybrid adsorption refrigeration system with ACB serving an office. Solar energy is collected to supply to the adsorption refrigeration and the desiccant dehumidification through regenerative water and desiccant water respectively. Auxiliary heaters are involved whenever the required driving temperatures are not sufficient. The adsorption chiller provides chilled water to the chilled beams for sensible cooling, it also furnishes the chilled water to the supply air coil for supporting the desiccant dehumidification. The chilled beam valve and the supply air valve are used to control the required chilled water flow rate to the respective equipment. For the system with ACB, supply air fan is needed for induction of indoor air. However for PCB, no supply and return air fans, and the associated air ducts are required.

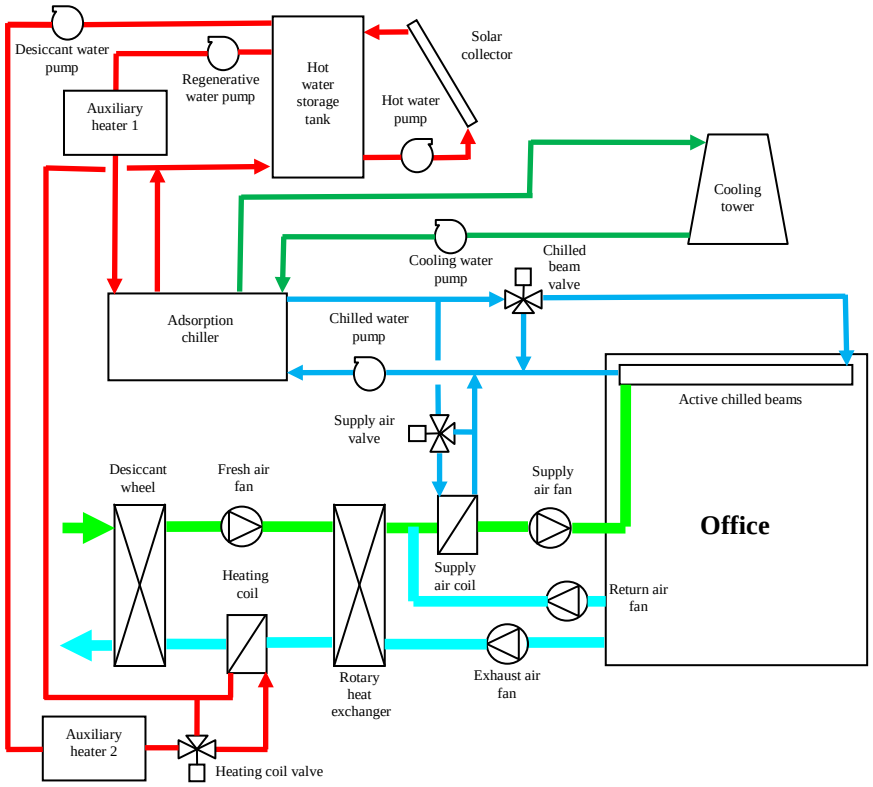

Fig. 1. Solar hybrid adsorption refrigeration system for active chilled beams.

2. Methodology

In this study, year-round dynamic simulation was applied for the solar hybrid adsorption refrigeration system. Generally the entire system model was built on the component-based simulation platform TRNSYS [6], and the validated component models of adsorption chiller [7] and desiccant wheel [8] were used. The models of ACB and PCB were developed from the empirical information of the manufacturers [9,10]. The other system components, including the office building zone, solar collector, storage tank, auxiliary heaters, rotary heat exchanger, water coils, cooling tower, pumps, fans and valves were based on those of TRNSYS and the component library TESS [11]. Different radiative load ratios were adjusted at the TRNSYS multizone building model. The indoor design conditions were set at 25.5°C and 60%RH. The floor area was 196 m^2 with 24 occupants and daily working schedule

between 08:00 to 18:00. The fresh air amount was based on 10 litres/s per occupant. The subtropical city Hong Kong (22.32°N and 114.17°E) was used, and the year-round dynamic simulation was carried out with the typical meteorological year for Hong Kong [12]. The major simulation parameters of the solar hybrid adsorption refrigeration system are summarized in Table 1.

Table 1. Values of major simulation parameters of solar hybrid absorption refrigeration system.

Fresh air stream		
Fresh air mass flow rate ($kg \cdot s^{-1}$)		0.288
Fresh air fan power (kW)		0.277
Exhaust air stream		
Exhaust air mass flow rate ($kg \cdot s^{-1}$)		0.259
Exhaust air fan power (kW)		0.166
Rotary heat exchanger		
Temperature effectiveness of rotary heat exchanger		0.8
Rotary heat exchanger power consumption (kW)		0.1
Desiccant wheel		
Mass per unit length of matrix material in desiccant wheel ($kg \cdot m^{-1}$)		0.003
Mass per unit length of silica gel in desiccant wheel ($kg \cdot m^{-1}$)		0.005
Half height or width of air channel (m)		0.0015
Outer diameter of desiccant wheel (m)		0.6
Effective area ratio of desiccant wheel		0.744
Fraction of wheel area for regeneration		0.5
Length of desiccant wheel (m)		0.2
Desiccant wheel speed (rph)		13
Number of discretization segments along the air channel length		20
Number of time steps for one revolution of the desiccant wheel		360
Desiccant wheel power consumption (kW)		0.1
Adsorption Chiller	**Typical**	**High-tech**
Number of stages per chiller	2	
Mass of metal in adsorption/desorption chamber per stage (kg)	60	80
Mass of silica gel in adsorption/desorption chamber per stage (kg)	30	40
Mass of metal in condenser coil per stage (kg)	75	90
Mass of metal in evaporator coil per stage (kg)	75	90
Maximum adsorbate intake in Freundlich equation	0.552	
Exponent in Freundlich equation	1.6	
Ratio of initial absorbrate intake to maximum abosrbrate intake	0.7	
Adsorption/desorption period (s)	360	

Cooling water system	**Typical**	**High-tech**
Cooling tower air volume flow rate ($m^3 \cdot s^{-1}$)	2.640	3.333
Cooling tower fan power (kW)	0.812	1.026
Cooling water mass flow rate ($kg \cdot s^{-1}$)	0.7	0.8
Cooling water pump power (kW)	0.138	0.168
Chilled water system	**Typical**	**High-tech**
Chilled water mass flow rate ($kg \cdot s^{-1}$)	1.05	1.3
Chilled water pump power (kW)	0.207	0.277
Hot water system	**Typical**	**High-tech**
Hot water mass flow rate ($kg \cdot s^{-1}$)	2.55	3.15
Hot water pump power (kW)	0.200	0.294
Desiccant water pump flow rate ($kg \cdot s^{-1}$)	0.15	
Desiccant water pump power (kW)	0.011	
Regenerative water pump flow rate ($k\ g \cdot s^{-1}$)	1.2	1.5
Regenerative water pump power (kW)	0.145	0.184
Chilled beams	**Typical**	**High-tech**
Model of ACB used	DID600B-L-2-M/3000x3000 [9]	
Numbers of ACB used	24	32
Model of PCB used	36CBPB14 [10]	
Numbers of PCB used	42	54
Supply air stream (ACB only)	**Typical**	**High-tech**
Supply air mass flow rate (kg·s-1)	1.008	1.344
Supply air fan power (kW)	0.258	0.345
Return air stream (ACB only)	**Typical**	**High-tech**
Return air mass flow rate (kg·s-1)	0.72	1.056
Return air fan power (kW)	0.092	0.135

3. Results and discussion

3.1. Performance indicators

A number of performance indicators were used in this study, including solar fraction *SF*, coefficient of performance *COP* and primary energy consumption *PE*, as determined below.

$$SF = \frac{Q_{sol}}{Q_{sol} + (Q_{aux1} + Q_{aux2})} \quad (1)$$

where Q_{sol} is the solar thermal gain, Q_{aux1} and Q_{aux2} are the heat output from Auxiliary Heaters 1 and 2 respectively.

$$COP = \frac{Q_e}{Q_g} \quad (2)$$

where Q_e is the refrigeration effect of absorption chiller and Q_g is the heat input to generator of absorption chiller.

$$PE = PE_p + PE_f + PE_{aux} \quad (3)$$

where PE_p is the primary energy consumption of pumps, PE_f is the primary energy consumption of fans, cooling tower, desiccant wheel and rotary heat exchanger, PE_{aux} is the primary energy consumption of auxiliary heaters.

In addition, the annually averaged room conditions, including zone temperature T_z and zone humidity RH_z, were also examined.

3.2. Solar fraction and coefficient of performance

Table 2 summarizes the annually averaged performances of the solar hybrid adsorption refrigeration system with different types of chilled beams for typical and high-tech offices. Generally the system could maintain satisfactory indoor conditions for both types of offices. The results of the typical office shows that the annually averaged *SF* of the system with PCB would become better, increased by 10.9% along with *R* decreased from 0.3 to 0.1, while that with ACB could be increased by 3.9%. Similarly for the high-tech office, the annually averaged *SF* of the system with PCB was raised by 15.6% for *R* from 0.3 to 0.1, and that with ACB by 6.4%. *SF* decreased with an increase of *R*, it was because the radiative load had less effect in reducing the zone air temperature. Hence, with a higher radiative load ratio, the zone air temperature would drop slower, meaning that the running hour of the chiller would increase. As such, the regenerative heat required was larger and resulted in a lower *SF*. For *COP*, although it was slightly increased with the rise of *R*, the change was minimal for both types of offices. At the same *R*, PCB had higher *COP* than ACB. The main reason was due to a higher chilled water supply temperature would be offered by the PCB, and the regenerative heat demand could be reduced.

Table 2. Annually averaged performance of solar hybrid adsorption refrigeration system.

Office	Chilled beams	*R*	*SF*	*COP*	T_z (°C)	RH_z (%)
Typical	ACB	0.1	0.689	0.548	25.02	53.12
	ACB	0.2	0.675	0.548	25.07	52.94
	ACB	0.3	0.663	0.548	25.13	52.80
	PCB	0.1	0.791	0.557	25.29	53.14
	PCB	0.2	0.754	0.558	25.39	53.09
	PCB	0.3	0.713	0.559	25.51	52.95
High-tech	ACB	0.1	0.568	0.546	25.19	52.51
	ACB	0.2	0.553	0.546	25.25	52.33
	ACB	0.3	0.534	0.547	25.33	52.07
	PCB	0.1	0.659	0.554	25.45	53.00
	PCB	0.2	0.616	0.554	25.56	52.87
	PCB	0.3	0.570	0.557	25.71	52.57

Fig. 2 illustrates the annual profiles of *SF* of the solar hybrid adsorption refrigeration system using ACB and PCB for both typical and high-tech offices at various *R*. The changing patterns were similar, with high *SF* from November to February and low *SF* from May to September. The former period was typical short autumn and winter in subtropical climate, while the latter was typical long summer. As compared between Fig. 2(a) and 2(b), the *SF* profiles of the typical office were generally higher than those of the high-tech offices, since the cooling demand of the typical office was lower and the involvement of auxiliary heaters would be less.

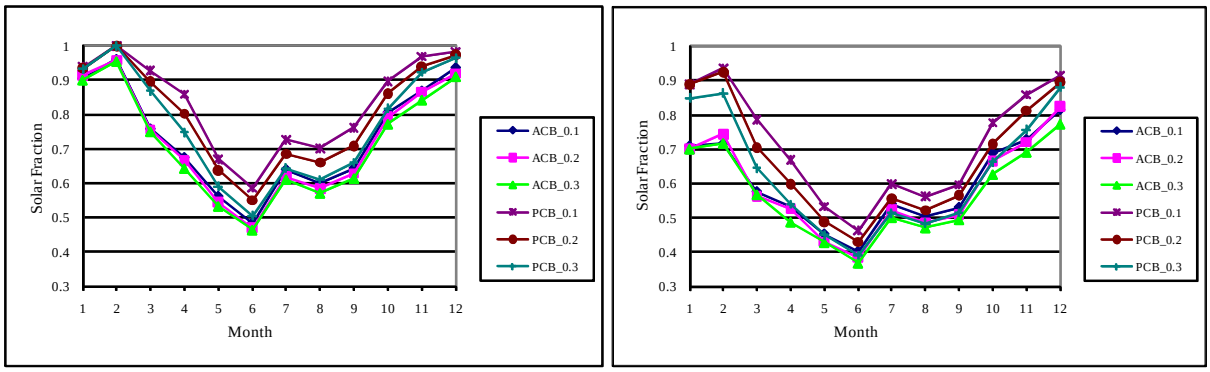

(a) Typical office *(b) High-tech office*

Fig. 2. Annual SF profiles solar hybrid adsorption refrigeration system.

Fig. 3 presents the annual profiles of *COP* of the adsorption chiller for ACB and PCB for typical and high-tech offices at various *R*. Generally the *COP* was higher in the winter months, while lower in the summer months. However the variation range of *COP* was narrow and maintained within about 10% even for different scenarios, since the chiller was supported by auxiliary heating. As compared between the chiller for the typical office and that for the high-tech office, although the latter *COP* was higher in the winter months, it was lower in the summer months. As a whole, the adsorption chiller for the high-tech office had lower annually averaged *COP* already shown in Table 2.

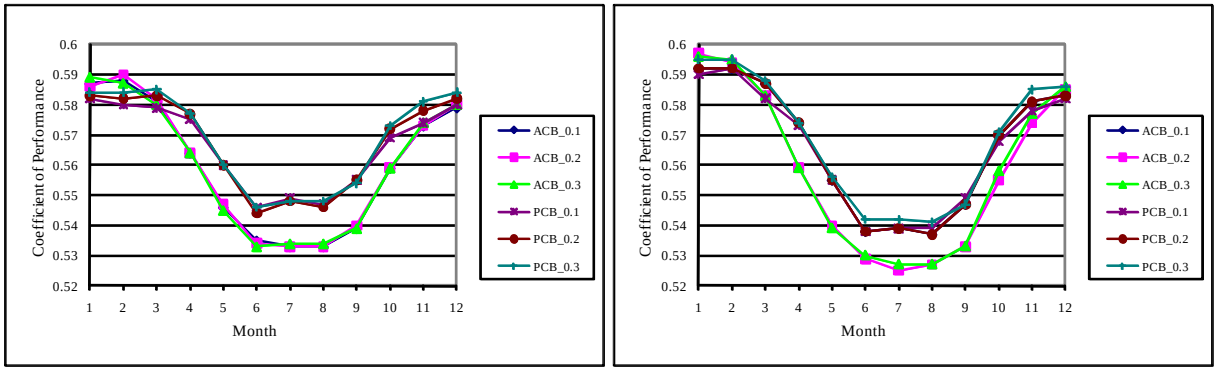

(a) Typical office *(b) High-tech office*

Fig. 3. Annual COP profiles of adsorption chiller of solar hybrid system.

3.3. Primary energy consumption

Table 3 summarizes the annual primary energy consumption of the solar hybrid adsorption refrigeration system with ACB and PCB for both typical and high-tech offices. The results of the typical office shows that the *PE* of the system with PCB would become less, reduced by 25.5% along with the decrease of *R* from 0.3 to 0.1, while that with ACB could be reduced by

8.0% only. Similarly for the high-tech office, the *PE* of the system with PCB was trimmed by 25.6% for *R* from 0.3 to 0.1, and that with ACB by 9.6%. These changing patterns were directly related to those of *SF*, since higher *SF* of the solar hybrid adsorption refrigeration system indicated less demand of auxiliary heating, thus leading to lower *PE*. At the same *R*, PCB could have less *PE* than ACB, up to 36.4% and 31.0% for typical office and high-tech office respectively. This was because the *SF* of the system with PCB was better than that with ACB, as discussed in Section 3.2, and the PE_{aux} of the system with PCB was less. In addition, the system with PCB did not have the additional supply and return air fans, so the PE_f of PCB was only about half of that of ACB.

Table 3. Annual energy performance of solar hybrid adsorption refrigeration system.

Office	Chilled beams	*R*	*PE* (kWh)	PE_p (kWh)	PE_f (kWh)	PE_{aux} (kWh)
Typical	ACB	0.1	60,943	19,466	8,232	33,247
	ACB	0.2	63,687	19,910	8,236	35,543
	ACB	0.3	66,212	20,155	8,238	37,820
	PCB	0.1	38,786	15,454	4,355	18,977
	PCB	0.2	44,764	16,588	4,361	23,815
	PCB	0.3	52,024	17,769	4,374	29,882
High-tech	ACB	0.1	94,371	26,124	9,670	58,578
	ACB	0.2	98,591	26,411	9,673	62,507
	ACB	0.3	104,398	26,971	9,676	67,751
	PCB	0.1	65,073	21,423	4,392	39,258
	PCB	0.2	75,309	22,871	4,402	48,036
	PCB	0.3	87,459	24,168	4,410	58,882

Fig. 4 presents the annual profiles of *PE* of the system with ACB and PCB for the two types of offices. Obviously the *PE* variation followed the seasonal change, and the system serving the high-tech office would demand higher *PE*. For the same type of chilled beams, higher *R* would require higher *PE*.

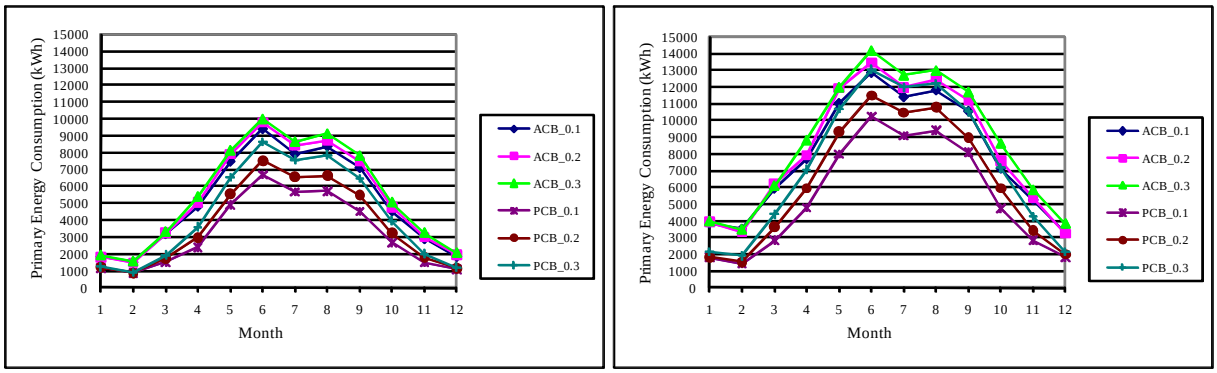

(a) Typical office *(b) High-tech office*

Fig. 4. Annual PE profiles of solar hybrid adsorption refrigeration system.

4. Conclusion

Through the year-round study of the solar hybrid adsorption refrigeration system using the two types of chilled beams, the effect of *R* on the system performances was investigated,

particularly the *SF* and the *PE*. It was found that the system with either ACB or PCB could have higher *SF* and lower *PE* when *R* was decreased from 0.3 to 0.1. Although both ACB and PCB could provide satisfactory indoor conditions for the typical and high-tech offices, the PCB had better annually averaged *SF* and total *PE* at the same *R*. As the conventional *R* of ACB is 0.1 or less, and that of PCB is between 0.1 and 0.2, suitable equipment selection and control provision of the solar hybrid adsorption refrigeration system would be technically feasible for office use in the hot and humid city. Through appropriate system design and year-round evaluation of solar air-conditioning, this would certainly help to determine a solution for reduction of carbon footprint of buildings in the subtropical climate.

Acknowledgement

The work described in this paper was fully supported by a grant from City University of Hong Kong (Strategic Research Grant, Project No. 7008037).

References

[1] H-M. Henning, Solar-Assisted Air-Conditioning in Buildings, A Handbook for Planners. Springer-Verlag Wien New York, 2004.

[2] U. Eicker, Solar Technologies for Buildings. Chichestor: Wiley, 2003.

[3] D. Song, T. Kim, S. Song, S. Hwang, S. Leigh, Performance evaluation of a radiant floor cooling system integrated with dehumidified ventilation, Applied Thermal Engineering, 28, 2008, pp. 1299-1311.

[4] J.L. Niu, L.Z. Zhang, H.G. Zuo, Energy savings potential of chilled-ceiling combined with desiccant cooling in hot and humid climates, Energy and Buildings, 34, 2002, pp. 487-495.

[5] K.F. Fong, C.K. Lee, T.T. Chow, Z. Lin, L.S. Chan, Solar hybrid air-conditioning system for high temperature cooling in subtropical city. Renewable Energy, 35(11), 2010, pp. 2439-2451.

[6] TRNSYS 16, a TRaNsient SYstem Simulation program. The Solar Energy Laboratory, University of Wisconsin-Madison, June 2006.

[7] S.H. Cho and J.N. Kim, Modeling of a silica gel/water adsorption-cooling system, Energy, 17, 1992, pp. 829-839.

[8] X.J. Zhang, Y.J. Dai and R.Z. Wang, A simulation study of heat and mass transfer in a honeycombed rotary desiccant dehumidifier, Applied Thermal Engineering, 23, 2003, pp. 989-1003.

[9] TROX Active Chilled Beams, Type DID600B-L-2-M/3000x3000, TROX Technik, TROX GmbH, July 2006.

[10] Carrier Product Data, Active and Passive Chilled Beams, model 36CBPB14, Carrier Corporation, 2008.

[11] TESS Component Libraries – Version 2.0. The Thermal Energy System Specialists, Nov 2004.

[12] A.L.S. Chan, T.T. Chow, S.K.F. Fong and J.Z. Lin, Generation of a typical meteorological year for Hong Kong, Energy Conversion and Management, 47, 2006, pp. 87-96.